Scale-Up of Agitated Drying: Effect of Shear Stress and Hydrostatic Pressure on Active Pharmaceutical Ingredient Powder Properties

Brenda Remy, Weston Kightlinger, Eric M. Saurer, and Nathan Domagalski
Late Phase Chemical Development, Bristol-Myers Squibb Co., New Brunswick, NJ 08903

Benjamin J. Glasser
Dept. of Chemical and Biochemical Engineering Rutgers University, Piscataway, NJ 08854

DOI 10.1002/aic.14669
Published online November 15, 2014 in Wiley Online Library (wileyonlinelibrary.com)

Scale-up of agitated drying processes to minimize particle size changes in active pharmaceutical ingredients (API) can be challenging. Particle agglomeration or attrition problems due to agitated drying are often discovered on the initial scale-up from the lab to the plant. Traditional laboratory drying equipment has not successfully reproduced the degree of agglomeration or attrition observed at scale. This discrepancy may be attributed to the ability of particulate solids, such as crystalline API's to transfer stresses from the normal direction into the shearing direction. As batch size increases during scale-up, the compressive and shearing forces experienced by the API increase. To overcome this limitation, a modified laboratory setup was constructed which reproduces the range of hydrostatic pressures observed during scale-up. This work highlights the use of the modified setup to characterize the propensity for particle attrition to occur at different stages of the drying process by measuring impeller torque. Torque measurements of the API powder at different hydrostatic pressures revealed a behavior consistent with Coulomb's law of friction. The torque data obtained from these measurements were used to determine the bulk friction coefficient for API powder beds at different liquid content. Additionally, the amount of work done by the impeller blades was correlated to the degree of particle attrition observed. A workflow for assessing risk of API attrition at scale is described. © 2014 American Institute of Chemical Engineers *AIChE J*, 61: 407–418, 2015

Keywords: active pharmaceutical ingredient, agitated drying scale-up, powder rheology, particle attrition

Introduction

A large portion of commercial pharmaceutical products involve oral dose formulations. The physical properties of the active pharmaceutical ingredient (API) in this type of formulation can often impact drug product performance.[1] In particular, the particle-size distribution of the API can have an effect on the stability, bioavailability, dissolution rate and content uniformity of the drug product, and on the reproducibility of the manufacturing process.[2] As such, great care is taken during the production of the API to achieve a targeted particle-size distribution. Control of the API particle-size distribution is traditionally achieved via batch crystallization processes[1] or by milling.[3] A significant amount of effort goes into designing crystallization and milling processes that consistently produce the desired API properties on scale-up.[4] The goal of the isolation and drying operations is then to further purify the API while preserving the particle-size distribution achieved upstream. However, the API particle-size distribution can also be affected by the drying process. Particle size alterations can occur during drying due to particle attrition[5] and agglomeration.[6,7] These phenomena are most prevalent in agitated dryers as particles are often subjected to large compressive and shearing forces. At the same time, agitated dryers can improve heat and mass transfer thus reducing the time needed for the drying operation. They are, therefore, commonly used in the manufacturing of API's. Additionally, agitated filter dryers have the advantage of combining the filtering and drying operations in one piece of equipment thus decreasing the occupational exposure to the API during manufacturing.

Scale-up of agitated drying processes to minimize particle attrition and agglomeration has been problematic in the pharmaceutical industry.[6] Particle size changes during drying are often discovered on the initial scale-up from the lab to the plant. Several factors can influence the degree of attrition or agglomeration observed at scale. Operating parameters such as agitation rate, liquid content of the particle bed, drying temperature, and pressure can have an effect on particle-size distribution.[8–10] Equipment configuration such impeller blade design and angle of the walls can lead to differences in particle size changes across equipment.[11–14] Material properties such as the crystal morphology and crystal strength of the API have been found to affect the degree of attrition

Correspondence concerning this article should be addressed to B. Remy at brenda.remy@bms.com.

observed during agitated drying.[15] These complexities have made the scale-up of agitated drying processes challenging.

Traditional laboratory drying equipment has not successfully reproduced the degree of agglomeration or attrition observed at scale. At the heart of this problem is the characteristic of particulate solids, such as crystalline API's, to transfer stresses from the normal direction into the shearing direction.[16] As such, the shearing and compressive forces experienced by the particles change dramatically during scale-up. Remy et al.[17] demonstrated this phenomenon via Discrete Element Method (DEM) simulations of bladed mixers at different scales. The authors found that, above a critical scale, normal and shear stress profiles scale linearly with the total weight of the particle bed. These results suggest that, to reproduce the shear stresses observed at scale, the same normal stresses or hydrostatic pressure experienced at scale must be applied in the lab. As laboratory units are design to use a small amount of material ($\sim$ 10 to 100 g), the hydrostatic pressure typically observed in traditional laboratory drying equipment is orders of magnitude lower than at scale.

To overcome this limitation, Lamberto et al.[18] constructed a laboratory setup which reproduced the range of hydrostatic pressures observed at scale. The setup consisted of a small cylindrical unit mechanically agitated by an impeller in which a normal load is applied by placing a weight on top of the particle bed. The authors developed a standardized protocol to test the propensity for attrition of API particles at scale with the modified laboratory setup. Based on the degree of attrition observed in the lab unit, an API would be classified as having a high, medium, or low risk for attrition during scale-up. With this methodology, the degree of attrition observed in the lab was the same order of magnitude as what was observed at scale for several API's. Following this work, am Ende et al.[19] used a similar setup as a screening tool to determine the propensity of API's to undergo attrition or agglomeration during agitated drying. The authors also used impeller torque data from a lab scale mixer to characterize agglomeration risk for powder beds with different levels of wetness. A ranking scale, based on the impeller torque data, was developed which characterized the risk of agglomeration at scale.

The studies done by Lamberto et al.[18] and am Ende et al.[19] are the first reported in the literature to mimic in the lab the degree of attrition and agglomeration observed during scale-up. The experimental procedures developed in these studies can inform the risk of attrition and agglomeration at scale and serve as screening tools. In terms of scale-up, it would be advantageous to have a laboratory tool that could mimic and potentially predict the behavior of the powder bed at larger scales. Specifically, developing tools which can provide understanding of the underlying physics of the behavior and delineate the relationship between API material properties and the tendency for attrition (or agglomeration) are goals in this work. We build on the findings of Lamberto et al. and am Ende et al. and describe a new methodology for predicting the degree of attrition during scale-up from knowledge of API material properties. A similar lab setup to the one developed by Lamberto et al. was used in this work to reproduce the magnitude of the hydrostatic pressure observed at scale. Torque measurements were used to correlate the amount of shear stress experienced by the API particles to the degree of attrition. Torque data were also used to measure the bulk friction coefficient for API powder beds with different levels of wetness. This information was then used to build a correlation between the amount of work done by the impeller blades and the degree of attrition at scale. A Bristol-Myers Squibb API currently in clinical development was used as the test material to demonstrate this methodology.

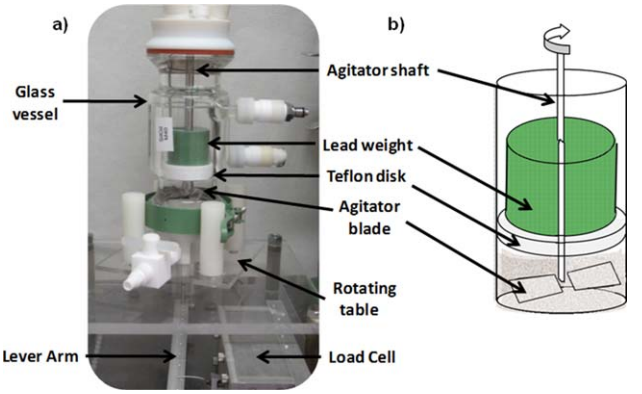

Figure 1. Laboratory setup.

(a) Photograph of equipment and (b) schematic of agitated glass vessel. [Color figure can be viewed in the online issue, which is available at wileyonlinelibrary.com.]

Experimental Method

Experimental setup

The laboratory unit used for this work is shown on Figure 1. It consists of a glass cylindrical vessel agitated by an impeller with two blades pitched at a 60° angle. The cylinder has an internal diameter of 60 mm, an internal height of 170 mm, and a volume of 500 mL. The height of the blades is 15 mm, and the diameter of the blades 55 mm. The clearance of the blades from the bottom of the cylinder is approximately 10 mm. A Teflon disk is inserted through the impeller assembly and weights are place on top of the disk. The Teflon disk sits on top of the API powder and distributes the normal load onto the particle bed during agitation to mimic the hydrostatic pressure experienced at scale. Table 1 shows the typical range of hydrostatic pressure experienced by API particles as the drying process is scaled from the lab to the pilot plant and ultimately to the commercial scale. The values shown in Table 1 were calculated using the equipment sizes used at Bristol-Myers Squibb during agitated drying scale-up. The size and number of weights applied to the API powder can be modified in the laboratory setup to simulate the range of pressures listed in Table 1.

In this setup, torque is measured using a load cell attached to a metal arm that pivots around a rotating table in which the glass vessel assembly sits as shown in Figure 1. As the blades move through the powder bed, the rotation of the

Table 1. Range of Hydrostatic Pressures Experienced by the API Powder During Scale-Up of Agitated Drying

Scale	Pressure (kPa)
Traditional lab scale dryer (50 g)	0.2
Pilot plant dryer (150 kg)	1.4
Commercial scale dryer (500 kg)	3.0
Modified Lab scale dryer (50g)	0.2–3.6

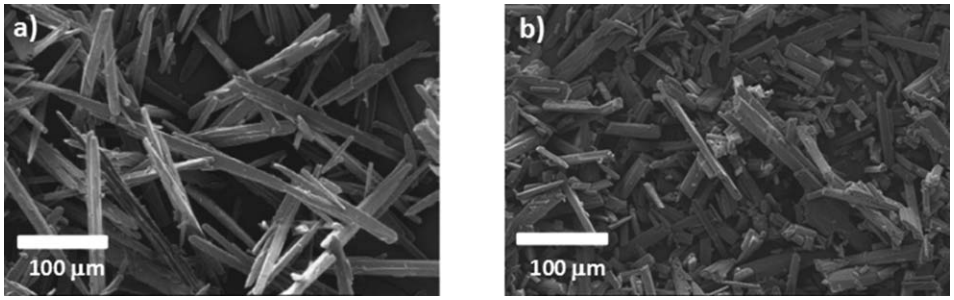

Figure 2. SEM pictures of API before and after drying (pilot plant).

(a) API before agitated drying; bulk powder density = 0.1 g/mL and (b) API after agitated drying; bulk powder density = 0.4 g/mL.

glass vessel causes the pivot arm to apply force on the load cell. Average torque is calculated by multiplying the measured force by the length of the pivot arm. In our work, the torque signal was recorded once every second. With this setup, the average shear stress experienced by the powder bed can be calculated from the equation given by Darelius et al.[20]

$$\langle \tau_{\theta r} \rangle = \frac{T}{2\pi R_{\text{cyl}}^2 H} \tag{1}$$

where $\langle \tau_{\theta r} \rangle$ is the average shear stress, T is the measured torque, R_{cyl} is the radius of the glass vessel and H is the total height of the powder bed when the blades are rotating. As torque can be correlated to shear stress by the equation given above, knowledge of agitator torque throughout the drying process could, in principle, be used to determine whether particles size changes are occurring. It should be noted that the torque measuring setup used in this study does not allow for direct measurement of torque during dynamic drying experiments. The jacket connections for the glass vessel would prevent the torque table (on which the vessel sits) from moving freely. For this study, we performed a number of agitation experiments for particle beds at room temperature and constant bed wetness (dry and wet particle beds). Although this represents an approximation of the drying process, it provides a way of studying the effect of liquid content on shearing of the powder bed and separates it from the effect of drying rate and temperature. This method can also be used to indicate when particle size changes are most likely to occur as a function of liquid content; information which is useful when designing the agitation protocol during scale-up of the drying process.

A Bristol-Myers Squibb API currently in clinical development was used as the test material for this study. This API had been shown to undergo a significant amount of attrition during agitated drying at the pilot plant scale. As such, it provided a good test material for laboratory attrition studies. Images of the API particles before and after agitated drying are shown in Figure 2. These images were obtained using a Scanning Electron Microscope (SEM). Figure 2a shows that the API particles before agitated drying have a long aspect ratio with a "rod-like" morphology. The long aspect ratio leads to a low bulk density powder when these API particles are dried in a tray drier without agitation (0.1 g/mL). When this material undergoes agitated drying, the particles break mostly length wise leading to shorter particles with lower aspect ratios as can be seen from Figure 2b. The lower aspect ratio of the agitated dried material leads to a higher bulk density after agitated drying (0.4 g/mL). It should be noted that particle agglomeration was not observed for this API during agitated drying at scale. As such, this material provides the opportunity to study particle attrition due to agitation while decoupling it from particle agglomeration.

At the start of each experiment, the powder is charged into the glass vessel from the top while the agitator blades are located at the bottom. A total of 50 g of API were used per experiment. Once the powder is charged, the Teflon plate is lowered to the top of the powder bed and the lead weights are placed on top of the Teflon plate. The powder is then agitated at 15 RPM until the torque signal reaches steady state (normally between 30 and 60 min of agitation). Agitation is then stopped; the lead weights and Teflon plate are taken off carefully without disturbing the powder bed. The part of the powder bed that is not within the height of the blades is removed leaving the portion of the powder bed within the span of the blades. A sample is taken from the powder bed within the span of the blades and analyzed for particle-size distribution using laser diffraction measurements. A wet dispersion method was developed and qualified for particle size measurements of the test material API ensuring sufficient solids suspension in the analysis chamber and minimal particle breakage during measurements.

Dry and wet powder beds were tested in this study. Powder beds were considered to be dry when their solvent content was below 0.5 wt% as measured by a Loss on Drying (LOD) test. Wet powder beds in this study have LOD values above 1.0 wt% and are wet with *n*-heptane. The solubility of the test material API in *n*-heptane is less than 1.0 mg/mL ensuring no dissolution of the API material into the solvent phase during the experiments. Agitation studies were conducted at different LOD levels for wet powder beds. The wet powder beds are tray dried prior to the agitation studies until the desired LOD level is reached. The wet powder is then loaded into the glass vessel and the procedure outlined before is followed.

The experimental data shown in this work were obtained using a fixed agitation rate of 15 RPM. Agitation studies at different agitation rates were conducted for blade speeds ranging from 10 to 100 RPM. These experiments showed that agitator torque is constant within this RPM range when torque is plotted against the number of impeller revolutions. This behavior suggests a quasi-static flow regime in which momentum transfer is governed by frictional contacts within the particle bed and is independent of shear rates. These results are also consistent with DEM simulations which have shown a quasi-static flow regime for particle beds agitated in bladed mixers[21] at low RPM's; a geometry similar to agitated dryers. Agitation rates below 10 RPM could not be

achieved with our experimental setup as the variable frequency drive used for this study was unable to control the agitation speed consistently in that range. The agitation rate of 15 RPM ensures that the flow occurs within the quasi-static regime. Additionally, this agitation speed is representative of the plant operating conditions.

Particulate Flows in the Quasi-Static Regime

Several characteristics of API powder beds during agitated drying are consistent with the behavior of particulate flows in the quasi-static regime. As such, a brief review of the rheology of quasi-static flows is provided. The rheological behavior of particulate solids is significantly different from that of molecular fluids. Although the dynamics of fluid systems are often adequately described by continuum treatments such as the Navier–Stokes equations, an equivalent set of equations for particulate systems is not readily available. The relationship between stress and strain rates is not well established due to the diverse behavior exhibited by particulate solids. A particle assembly may behave as a viscoelastic solid or as a liquid depending on the localized concentration and stress. When a granular material behaves as a viscoelastic solid, it is able to support large loads such as building foundations by distributing the load across frictional contacts within the particle bed.[22] In contrast, natural disasters such as avalanches and landslides occur when particles within a granular assembly move freely and independently from each other leading to a liquid-like behavior.

Particulate flows at high concentrations and low shear rates tend to fall in the quasi-static regime where particles experience sustained contacts with their neighbors and momentum transfer is governed by the forces generated from the particle-particle contacts.[23] In this regime, the frictional particle contacts give rise to a yield stress which must be overcome to induce flow.[24] At shear stress values below the yield stress, the particle assembly remains stationary and behaves as a rigid solid. When shear stresses are above the yield stress, the particle assembly begins to flow. During flow, the sustained contacts generate stresses which are independent of the rate of deformation (i.e., independent of agitation rate). The rate independence of the shear stress can be explained by considering that, at low shear rates, the average number of frictional contacts remains constant during flow.[25] The magnitude of shear stresses in the quasi-static flow regime is, however, proportional to the magnitude of the normal stress (or pressure) as described by Coulomb's law of friction[20]

$$\tau = \sigma \tan \varphi + C_f \tag{2}$$

where τ is the shear stress, σ is the normal stress and φ is the angle of internal friction. The $\tan \varphi$ term is referred to as the bulk friction coefficient of the material. The term C_f describes the cohesiveness of the material with positive values of C_f corresponding to cohesive materials while $C_f = 0$ for noncohesive systems. The C_f and $\tan \varphi$ terms in Eq. 2 are generally regarded to be characteristic properties of a material.

Results and Discussion

Characterization of attrition in dry material

We begin by characterizing the effect of agitation on particle attrition for dry powder beds. Initial scale-up of the agitated drying process for the test material API revealed that the most prominent effect of agitation was breakage of the particles lengthwise. Using our modified laboratory setup, we were able to follow the kinetics of particle breakage for this API in the laboratory. Figure 3a shows a typical torque vs. time curve for agitation of the dry API with 2.0 kPa of pressure; a pressure within the typical range observed in the larger scale equipment (see Table 1). Figure 3b shows the initial 300 s of the torque signal from Figure 3a. Figure 3c shows corresponding particle size distribution (PSD) profiles at various time intervals for this experiment. As the impeller blades begin to rotate, the torque signal spikes from 0 Nm to roughly 0.1 Nm in the span of a few seconds (Figure 3b). This initial spike in the torque is associated with the yield stress of the dry material. At torque values below the yield stress, the powder bed remains stationary and the material behaves like a rigid solid. Flow is induced once torque values are above the yield stress. A similar behavior was observed by Karmakar et al.[26] for soil beds at different moisture contents and it is consistent with the behavior of visco-plastic fluids.

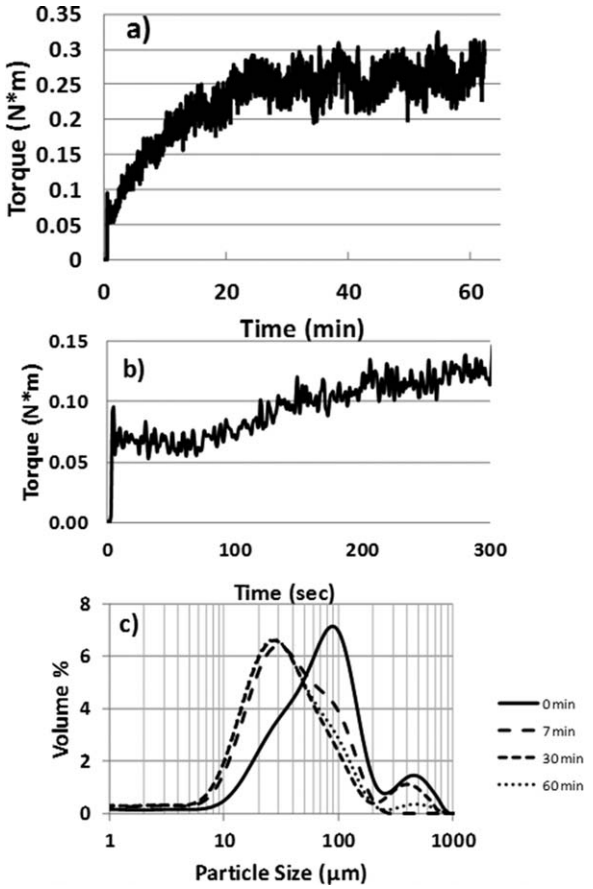

Figure 3. Torque profile and PSD for dry API with 2.0 kPa pressure applied.

Agitation conditions: 15 RPM for 60 min. (a) Torque profile, (b) Initial 300 s of the torque profile from Figures 3a, (c) particle-size distribution of API before agitation and after 7, 30, and 60 min of agitation.

After the initial spike in torque, the material yields and begins to flow. The magnitude of the torque then decreases from approximately 0.1 to approximately 0.05 Nm within a few seconds. However, once flow is induced, the torque signal increases until steady state is reached after roughly 30

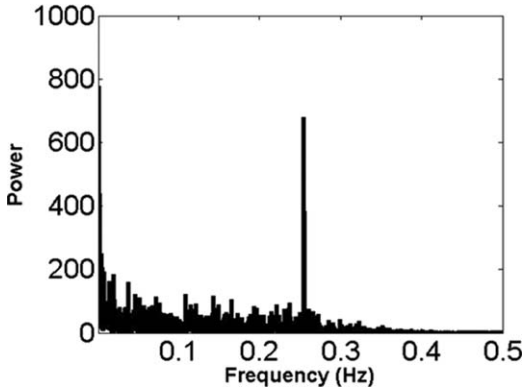

Figure 4. FFT Analysis of Torque profile after steady state is reached from Figure 3.

min of agitation (Figure 3a). The increase in torque is associated with the densification of the powder bed due to particle breakage. The mean particles size (D50) of the material prior to agitation was measured to be 65 μm ("0 min" PSD curve in Figure 3c). These long, rod-like particles trap a significant amount of air and pack very loosely leading to a low bulk density powder (~0.1 g/mL bulk density). During agitation, the shearing action of the blades begins to break the particles lengthwise leading to shorter particles that can pack better. After just 7 min of agitation, the mean particle size is reduced to 32 μm ("7 min" PSD curve in Figure 3c). As the particles break during agitation, a larger amount of energy is required to maintain flow as the number of frictional contacts within the powder bed increase due to densification of the material. The increase in energy needed to maintain flow is captured in the increase of torque. The plateau in the torque signal observed after 30 min was found to correspond to the end of the particle breakage process. Figure 3c shows very similar PSD profiles at 30 and 60 min of agitation with a mean particle size of 29 μm. The bulk density of the powder after the 60 min of agitation was measured to be approximately 0.4 g/mL; significantly higher than that of the input material and similar to the bulk density observed after agitated drying at the pilot plant scale. The PSD profiles and torque trends were found to be reproducible over several experiments at the conditions used for Figure 3.

Torque fluctuations can be observed in Figure 3a after the system has reached a steady state after 30 min of agitation. The torque signal fluctuates between 0.2 and 0.3 Nm. A Fast Fourier Transform (FFT) analysis of the torque signal at steady state revealed that the main frequency of the fluctuation is equal to the rotation frequency of the blades (0.25 Hz for a blade speed of 15 RPM). The power spectrum obtained from the FFT analysis in shown in Figure 4. These results are consistent with the DEM simulation results in bladed mixers reported by Remy et al.[21] where periodic pressure and shear stress fluctuations were observed throughout the particle bed. The torque fluctuations suggest that the material compresses when the blades are present and dilates in-between blade passes leading to higher particle breakage near the impeller blade. Fluctuations in torques at frequencies lower than the blade speed are also observed. These fluctuations are smaller in magnitude and can be attributed to slip-and-stick behavior as the particles flow past one another. It should be noted that blade speed did not have a significant effect on the mean and amplitude of the torque fluctuations. Instead, blade speed affected the frequency of the fluctuations suggesting that blade speed provides the time scale for the particle breakage process within the range of RPM studied (10–100 RPM).

The hydrostatic pressure/normal stresses experienced by the API particles increases significantly as the agitated drying process is taken from the laboratory to the plant. As shear stress scales with the pressure in the quasi-static regime,[24] it might be expected that attrition kinetics during agitated drying would be dependent on hydrostatic pressure. The effect of pressure on torque signal and on API PSD is shown in Figure 5. Figure 5a shows the torque profiles at three different hydrostatic pressures. It should be noted that the torque profiles shown in Figure 5a were obtained by applying a moving average filter in which the torque signal is averaged out over the course of 60 s. Figure 5b shows the PSD profiles obtained after 60 min of agitation at each pressure. The PSD of the starting material for these experiments is shown in Figure 5b. The lowest pressure case (0.2 kPa) represents the typical pressure achieved in a traditional lab agitated dryer for a 50 g experiment. At this pressure, the torque signal spikes initially as the yield stress is overcome and remains fairly constant throughout the course of the experiments while torque increases for the 1.1 and 2.0 kPa cases until a steady state is reached. Particle breakage was observed at the low pressure with the mean particle size decreasing from 65 to 47 μm (Figure 5b). However, the degree of attrition observed at the higher pressure settings (1.1 and 2.0 kPa) was significantly higher. The mean particle size for the higher pressure experiments (1.1 and 2.0 kPa) was approximately 28 μm after 60 min of agitation as can be seen from Figure 5b. These

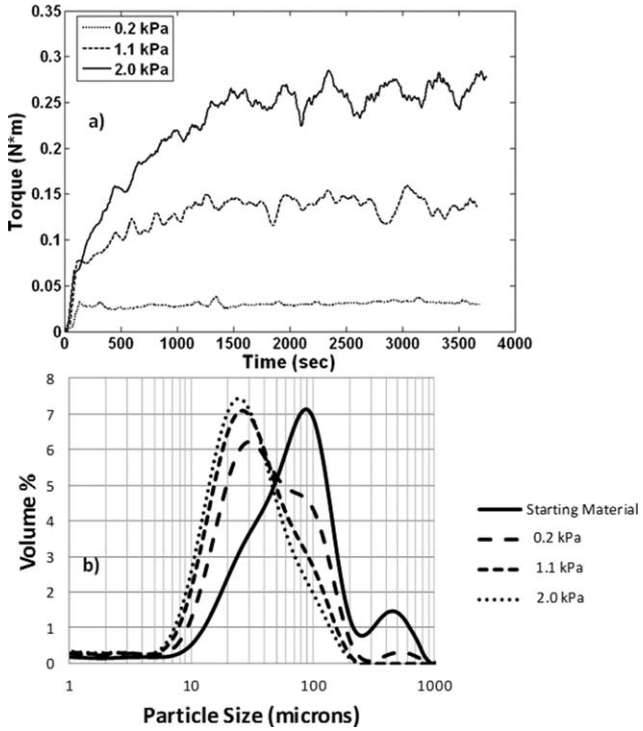

Figure 5. Effect of pressure on torque profile and PSD.

(a) Torque profile for dry API with pressures applied agitated at 15 RPM for 60 min, (b) PSD of API before agitation and after 60 min agitation at 15 RPM. Note: a moving average filter was applied to the data shown in Figure 5a. The plotted values represent an average of the torque over 60 s.

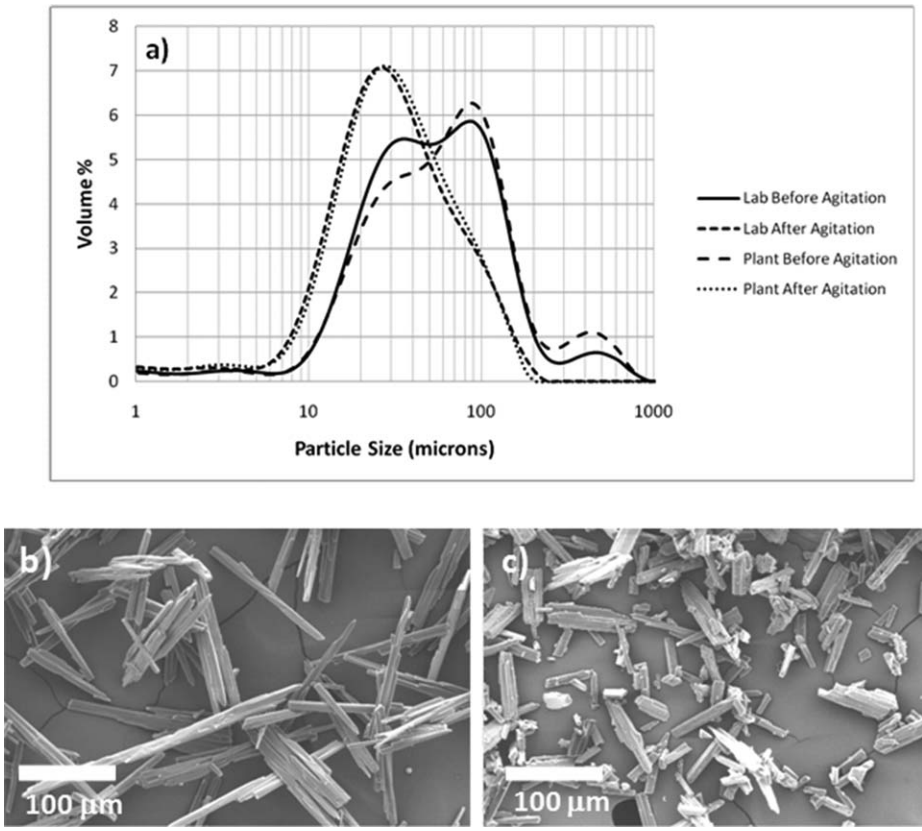

Figure 6. Comparison of lab attrition vs. pilot plant attrition.

(a) PSD for API dried in lab and pilot plant under similar pressure/# of blade passes, (b) SEM picture of lab API before agitation, and (c) SEM picture of lab API after agitation. Note: Plant material SEMs are shown in Figure 2.

results provide an explanation as to why traditional laboratory equipment has not consistently captured the propensity for attrition of API particles during agitated drying. The lower hydrostatic pressures which are typically achieved in the lab lead to shear stresses which are orders of magnitude lower than what the API particles experiences at scale.

The increase in torque observed at higher pressures is indicative of the densification of the material as the particles break. The bulk densities of the powders after the 1.1 and 2.0 kPa experiments were very similar at approximately 0.4 g/mL. A lower bulk density of 0.2 g/mL was obtained for the 0.2 kPa case suggesting that the flat torque signal is due to a lower degree of densification during agitation. The time for the torque signal to reach steady state was different at each pressure. Although steady state is reached within a few minutes for the 0.2 kPA case, steady state is reached around 20 min for 1.1 kPa and around 30 min for 2.0 kPa. The value of the torque at steady state at 1.1 kPa is roughly half of that at 2.0 kPa. This is consistent with Coulomb's law of friction which predicts a linear dependency of shear stress on normal stress.

Based on the results presented thus far, we hypothesized that the particle breakage observed in the pilot plant could be reproduced in the lab by matching the hydrostatic pressure experienced by the API particles at scale. Additionally, as torque was found to be independent of blade speed, the number of blade passes experienced by the API at scale was matched in the lab. Figure 6a shows a comparison of the particle-size distribution for the pilot plant and laboratory setup when the hydrostatic pressure and number of blade passes were matched (1.1 kPa and 510 blade passes). Figures 6b, c show SEM images of the lab material before and after agitation, respectively (SEM images for the pilot plant material are provided in Figure 2). As can be seen from these figures, for comparable starting materials, the laboratory test matched the entire particle-size distribution profile observed in the pilot plant. As the material is agitated in the lab under similar conditions as in the plant, the particles break mostly across their short axis leading to shorter particles which pack better than the starting material. The laboratory test was able to match the final bulk density of the powder obtained from the pilot plant dryer (~0.4 g/mL). These results suggest that, for materials in which particle attrition is the dominant mechanism during agitated drying, the resulting particle size can be predicted from laboratory scale experiments in which the pressure and number of blade passes are kept constant.

Characterization of Attrition in Wet Material

During drying, the powder bed is agitated under different levels of liquid content. Agitation is applied to promote heat and mass transfer and reduce the time needed for the drying operation. The presence of a liquid phase gives rise to different phenomenological behaviors in wet materials from what is observed in dry systems. The apparent friction and cohesion between particles change even with small amounts of liquid present, leading to changes in shear stresses as the wet material flows.[27] In this section, we characterize the degree of attrition observed in agitated API powder beds wet with *n*-heptane. As mentioned earlier, the API solubility in *n*-heptane is very low, preventing dissolution of the API in the liquid phase during the agitation experiments.

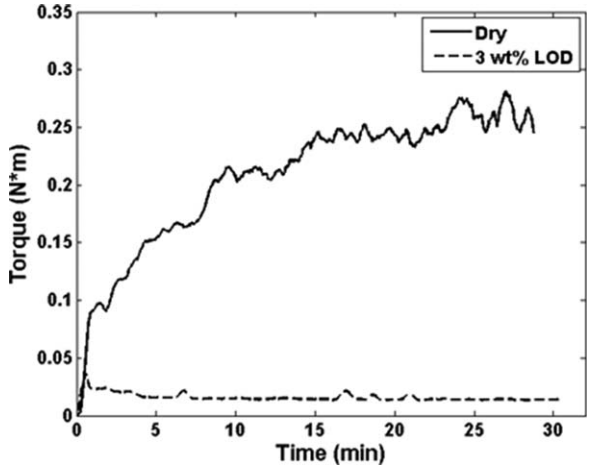

Figure 7. Effect of LOD on Torque (2.0 kPa, 30 min, 15 RPM).

Note: moving average filter applied to torque signal.

Torque profiles for dry API and wet API with 3% LOD are presented in Figure 7 for a hydrostatic pressure of 2.0 kPa. Several authors have shown that torque profiles for agitated particle beds change with the moisture content of the bed.[19,26] The results shown in Figure 7 are consistent with these observations from the literature. The increase in torque observed for the dry system is not present in the wet material torque signal. The magnitude of the torque is significantly less for the wet material. The torque signal for the dry material reaches a value of approximately 0.25 Nm while the torque signal for the wet material remains below 0.1 Nm throughout agitation. The lower torque signal suggests a lower degree of attrition (and densification) for the wet material. This is confirmed by the PSD profiles and SEM pictures presented in Figure 8. The PSD profile remains almost unchanged after 7 and 30 min of agitation at 3% LOD. As such, the bulk density of the wet material after agitation also remains low (~0.1 g/mL). Several reasons could lead to the lower torque and minimal particle attrition observed for the wet material. The liquid phase present in the wet system could act as a lubricant when the particles come in contact during flow. This lubrication effect could lower the apparent friction at the particle level thus lowering the amount of shear stress generated during agitation and minimizing the amount of particle breakage. Figures 8b, c offer an additional clue as to the effect of the liquid phase. When liquid is present, the thin rod-like particle can stack up along the main axis, forming agglomerates held together by cohesive forces. Formation of similar agglomerates in a wet bed of rod-like particles has been reported by Lekhal et al.[15] Similar to the effect of stacking wood lengthwise to form stronger wood composites, the formation of these API agglomerates can lead to an increase in crystal strength along the main axis thus reducing the tendency for the primary particles to break. It should be noted that these agglomerates are not preserved when the wet material is dried.

Wet particle beds with LOD ranging from 1% to 14% showed significantly lower torque and less particle attrition when compared to the dry material. Table 2 shows the effect of LOD on particle attrition for the test material API. The data shown in this table were collected by agitating API powder beds at 2.0 kPa for 60 min in the laboratory unit. The percent reduction in particle size was calculated by taking the difference between the mean particle size of the starting material and the mean particle size of the material after agitation and then dividing it by the mean particle size

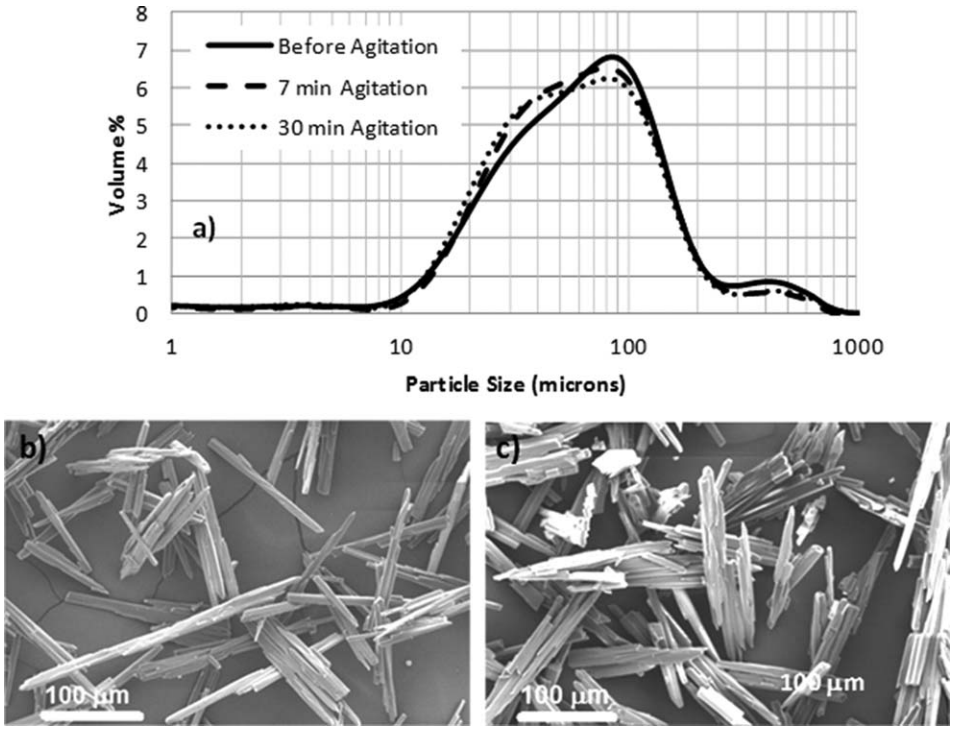

Figure 8. Effect of LOD on PSD and SEM.

(a) PSD of API before and after agitation (3.0% LOD, 2.0 kPa), (b) API SEM before agitation, and (c)API SEM after 30 min of agitation (3% LOD, 2.0 kPa).

Table 2. Effect of LOD on Particle Attrition: Data Generated with 2.0 kPa of Pressure

LOD (wt %)	Percent Reduction in Particle Size
14.0	1.8%
10.0	5%
3.0	14%
1.1	20%
<0.5	60%

of the starting material. At high levels of liquid content (14 wt %), almost no attrition occurs. The degree of attrition increases as LOD decrease. It should be noted that this behavior is API and material specific. There are several examples in the literature[18,19] that show wet API powders which are more susceptible to particle breakage than dry API powders. For the API used in this work, agitation of dry material results in higher attrition than agitation of wet material. For this API, a significant increase in particle attrition is observed when LOD decreases from 1.1% LOD to <0.5% (i.e., dry material). This suggests the existence of a critical liquid content level below 1.1% LOD. Above the critical liquid content, minimal particle attrition occurs and below it particles are more susceptible to attrition. The existence of critical wetness levels during drying has been previously reported by Lekhal et al.[8,15]

It could be argued that the decrease in torque observed for the wet material in the lab is a result of the decreased mobility of the particle bed in the lab apparatus under the higher pressures. The lab vessel diameter is significantly smaller than the diameter of the pilot plant unit and the presence of the lead weights could reduce the ability of the wet powder bed to dilate, rearranging the particle orientation and potentially leading to attrition. However, inspection of the impeller current draw data from the pilot plant unit suggests that this was not the case. Measurement of torque at the pilot plant scale was not possible due to equipment limitations. Impeller current provides a way to correlate impeller power draw to torque. Table 3 shows the current draw of the pilot plant impeller at different stages of the drying process. At the beginning of the drying process, when the LOD is higher, the impeller current draw is lower. As the material dries and the LOD is reduced, impeller current increases until it reaches a value of approximately 2.0 amps. These results are consistent with the torque data obtained in the lab which shows higher torque values for dry powder beds. Although particle size data throughout the pilot plant drying process are not available (particle size was only measured at the end of drying), the higher impeller current at lower LOD values suggests that most of the particle breakage occurred toward the end of the drying operation.

Figure 9 shows the effect of pressure on torque profiles for 1.1% wet API powder. A moving average filter was

Table 3. Effect of LOD on Impeller Current Draw During Agitated Drying at the Pilot Plant Scale

LOD (wt %)	Impeller Current (Amps)
3.2	1.2
1.4	2.1
<0.5	1.9

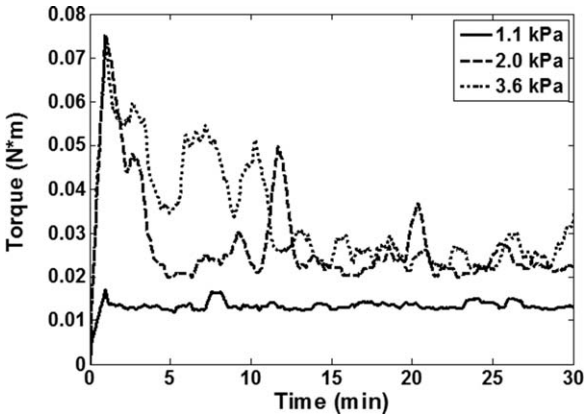

Figure 9. Effect of pressure on torque profile for wet material.

Torque profiles here are for 1.1 wt % LOD.

added to the torque data shown in Figure 9 where each data point represents the average torque obtained over the previous 60 s. The torque profiles observed at 1.1% LOD have some interesting features which offer insights into the rheology of wet API powders. At low hydrostatic pressures (<1.1 kPa), the torque profile is fairly flat, consistent with the behavior observed for 3% LOD. At the higher pressures, the torque signal reaches a peak value and then decreases until a steady value is reached which is lower than the peak torque. This is different from what was observed in dry API beds. The peak torque value, which is associated with the yield stress of the material, increases as hydrostatic pressure increases from 1.1 to 2.0 kPa for the 1.1% wet case. This behavior is consistent with the results reported by Karmakar et al.[26] for wet soils. The increase in yield stress indicates that wet powder beds have a higher resistance to flow at increased compression states. However, a similar value of peak torque is observed between 2.0 and 3.6 kPa. A possible explanation for this behavior is that, for wet API beds at high hydrostatic pressures, the dryer walls or the impeller blades can support some of the weight of the powder bed at the onset of flow (similar to the Janssen effect observed in silos). A similar behavior has been observed via DEM simulations of spherical particles in bladed mixers.[17] Once the yield stress is overcome and the material begins to flow, the lubrication effect of the liquid phase leads to a decrease in torque. Particle size measurements during the agitation experiments showed that particle breakage occurred before the steady state torque value was reached. Most of the attrition that was observed for the wet API experiments occurred within 15 min of agitation, suggesting that particle breakage in the wet powder bed is associated with the material yielding.

Knowledge of how impeller torque (and therefore shear stress) evolves throughout the drying process can be useful when operating agitated drying processes at scale. As we have shown that impeller torque can be correlated to changes in particle size, monitoring of torque (or impeller power draw) during scale-up could alert the operator of particle size changes occurring as drying takes place. The agitation protocol can be modified based on the torque signal during drying. If torque is low at the beginning of drying, when the material is wet, agitation may be maintained or increased to improve the drying rate. Once the torque signal begins to rise, indicating potential particle breakage, agitation rates

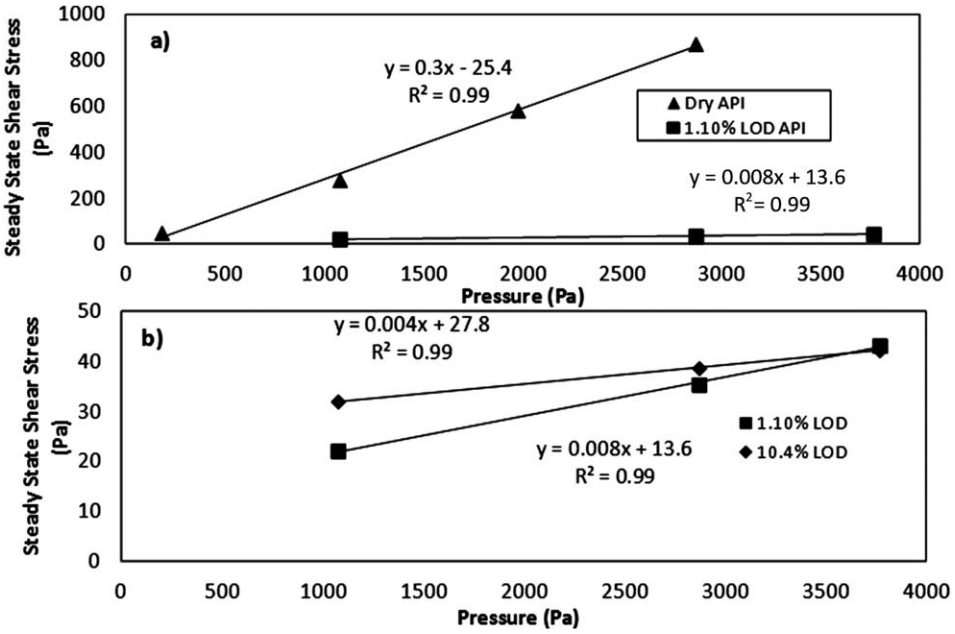

Figure 10. Bulk friction coefficients for wet and dry API powder beds.

could be reduced for the remainder of the drying process to preserve desired particle size.

Scale-Up of Agitated Drying to Minimize Attrition

For agitated drying processes at low RPM's, the relationship between shear stress and normal stress (or pressure) is given by Coulomb's law of friction. Shear stress scales linearly with normal stress times a constant called the bulk friction coefficient (see Eq. 2). The bulk friction coefficient is generally regarded to be a material property. As an estimate of the normal stress at scale can be easily obtained from a hydrostatic pressure calculation, knowledge of this material property can provide an estimate for the shear stress that API particles experience as the drying process is scaled. The laboratory setup used in this study allowed the measurement of bulk friction coefficients for API powder beds at different levels of liquid content. Figure 10 shows shear stress values obtained when the torque signal reaches steady state vs. pressure for dry and wet API. Figure 10a shows the data obtained for dry and 1.1% wet API while Figure 10b shows the data for 1.1% and 10.4% wet API. A linear relationship is observed for both dry and wet API beds consistent with the predictions from Coulomb's law of friction. We find that the bulk friction coefficient is dependent on the liquid content of the particle bed. The bulk friction coefficient for dry API is estimated to be approximately 0.3 (from the slope of the line drawn through the data) and is significantly higher than those measured for the wet API beds. This again speaks to the higher interparticle friction experienced by dry API particles during flow which leads to an increase in particle attrition. For the wet API beds, the bulk friction coefficient decreases as liquid content increases as can be seen from Figure 10b. These results support the hypothesis that the liquid phase present in wet API beds can act as a lubricant, reducing interparticle friction thus reducing the amount of attrition observed at these conditions. A positive y intercept is obtained for the 1.1% and 10.4% wet datasets. The positive value of this term indicates that the wet API particle beds are cohesive in nature, as expected. The cohesive values increase between the 1.1% case ($\sim$17 Pa) and the 10.4% case ($\sim$28 Pa). One might expect a y-intercept value for the dry API case close to zero. Although a negative value is observed in Figure 10a (~ -25 Pa), the magnitude of the y intercept is relatively small compare to the scale of the y axis data shown in Figure 10a (between 0 and 1000 Pa). Additionally, the 95% confidence interval of the y intercept from the linear regression of the dry API data passes through zero (-124.1 to 73.4) further suggesting that the y-intercept value is not significant. The small negative value obtained for this quantity is most likely due to experimental error in the dataset. It should be noted that the 95% confidence interval for the y intercept of the 1.1% and 10.4% LOD do not pass through zero.

Knowledge of the bulk friction coefficient as a function of liquid content provides only a portion of the information needed to ensure that attrition is minimized during agitated drying scale-up. A means of estimating the degree of attrition

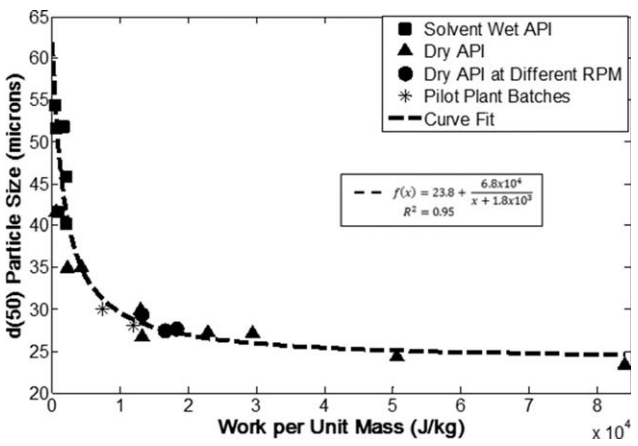

Figure 11. Work per unit mass vs. API particle size (d50).

Table 4. Range of Parameters Used for Generating the Particle Size vs. Impeller Work Curve (Figure 11)

Parameter	Min	Max
Static Pressure (kPa)	0.2	3.0
Solvent Content (LOD, wt %)	<0.5	14
Agitation Speed (RPM)	10	20

based on energy input by the impeller blades during agitation would also be useful. We generated a simple attrition curve that correlates the post-agitation particle size to the amount of work per unit mass done by the impeller blades. Figure 11 shows the median particle size (d(50)) vs. impeller work per unit mass for a wide range of processing conditions; including dry and solvent wet API as well as a range of hydrostatic pressures and impeller RPM's. Table 4 lists the range of parameters used to generate the data shown in Figure 11. Impeller work is calculated from impeller torque by the following equation

$$W = \int_0^t T \cdot \omega \, dt \tag{3}$$

where W is the work done by the blades over time t, T is the impeller torque, and ω is the angular velocity of the impeller blades. In Figure 11, we plot the total amount of work divided by the total mass experiencing the work. A plateau for large W per unit mass is obtained when a least squares fitting of the data is performed with a reasonable fit ($R^2 = 0.95$). The least squares fitting shows that the mean particle size approaches approximately 24 μm as impeller work increases. Figure 11 shows that all the data collected across multiple operating conditions collapses into a single attrition curve.

Once an attrition curve is generated, the amount of work per unit mass performed by the impeller at scale can be estimated from the bulk friction coefficient of the material at the different liquid levels. From knowledge of the drying batch size and the diameter of the agitated drier, a normal force can be estimated from a simple hydrostatic pressure relationship. Shear stresses at the different stages of drying can be estimated from the bulk friction coefficients, which in turn can be used to calculate impeller torque. The torque estimate can then be used to estimate the amount of work per unit mass done by the impeller of the larger scale agitated drying unit. In Figure 11, we have plotted the pilot plant particle size data vs. an estimate of the work per unit mass for two different pilot plant batches. As can be seen from Figure 11, the attrition curve provided a good estimate for the pilot plant particle size data. In addition to the two pilot plant batches shown in Figure 11, three additional pilot plant batches were run under aggressive agitation conditions expected to yield work per unit mass $> 8.0 \times 10^4$ J/kg. The mean particle size for these three batches ranged between 22 and 25 μm. This is consistent with the prediction from the laboratory data of the particle size reaching a plateau of approximately 24 μm for high values of work per unit mass. These results suggest that the resulting particle size for a particular agitation protocol can then be estimated from an attrition curve generated in the lab. If the amount of attrition is too high for a particular agitation protocol, the agitation rate and/or agitation time can be adjusted to minimize attrition.

Figure 12 summarizes a workflow for estimating particle attrition at scale from the bulk friction coefficient and the attrition curve determined in laboratory studies. The workflow is described below:

1. Begin by estimating the pressure inside the large-scale dryer via a hydrostatic pressure approximation from knowledge of the batch size and the dryer diameter.

2. From the bulk friction coefficient at a given LOD, estimate the shear stress expected at scale when agitating at a specific LOD.

3. From the shear stress, estimate the amount of torque generated during agitation at a specific LOD from the following equation

$$T = 2\pi R_{\text{cyl}}^2 H \langle \tau_{\theta r} \rangle \tag{4}$$

4. Estimate the amount of work per unit mass from the torque during agitation at a specific LOD using Eq. 3.

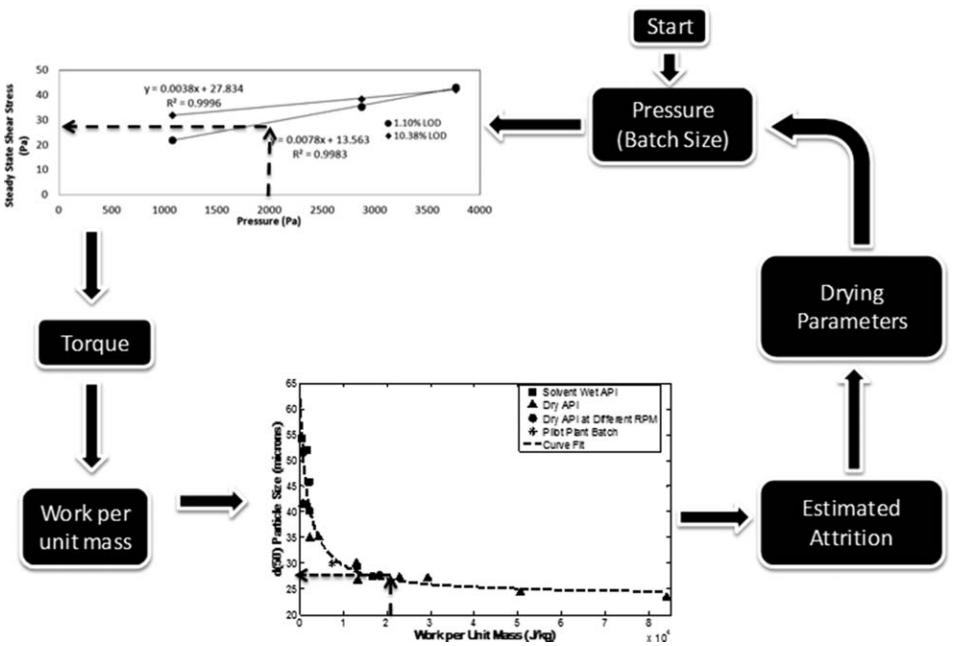

Figure 12. Workflow for scale-up of agitated drying.

Table 5. Lab Attrition vs. Pilot Plant Attrition for Other API's: Comparison of Pilot Plant vs. Lab Attrition for Other API's Following the Methodology Outlined in This Article

Compound	Morphology	Mean Particle Size—Before Agitation (μm)	Mean Particle Size—After Plant Agitation (μm)	Mean Particle Size—After Lab Agitation (μm)
API 1	Rod-like	65.0	28.1	28.7
API 2	Agglomerates	86.9	46.0	42.0
API 3	Thin needles	15.4	12.3	10.3

5. Repeat Steps 1–4 for every LOD for which the API powder is agitated until the drying specification is met.

6. Calculate the total amount of work per unit mass from Steps 1–5. From the particle size vs. work per unit mass curve generated in the lab, estimate the resulting particle size after agitation.

7. If the amount of attrition estimated from Steps 1–6 is acceptable at the end of drying, the agitation protocol at the different LOD stages can be implemented at scale. If the estimated attrition is too high, the drying parameters may need to be adjusted. For example, it may be necessary to reduce the amount of agitation used as the API dries through certain ranges of solvent content (LOD).

8. Repeat Steps 1–7 until an acceptable agitation protocol is identified.

The workflow proposed in this article has been tested with two additional API's currently in development at Bristol-Myers Squibb. Table 5 shows the comparison between the attrition observed at the pilot plant scale vs. attrition observed in the lab. The material particle size prior to agitation is similar for the pilot plant and lab batches shown in Table 5. API 1 represents the test material used for the work described in this article. The API 2 and API 3 pilot plant batches were run under aggressive agitation conditions leading to work per unit mass values beyond the particle size plateau predicted from the laboratory data. The laboratory data for API 2 and API 3 listed in Table 5 also represent aggressive agitation conditions beyond the particle size plateau. As can be seen from Table 5, the mean particle size of laboratory batches matches well the mean particle size observed in the pilot plant for API's of different morphologies and initial particle sizes. This suggests that this workflow can have broad applicability when scaling agitated drying processes from the lab to the plant.

It should be noted that the assumption that normal stresses can be predicted by hydrostatic pressure may not be valid for all API's and equipment configurations. The equipment walls and impeller blades might support some of the weight of the particle bed once a critical bed height has been reached leading to lower pressures at the bottom than what is predicted from the hydrostatic approximation.[17] However, the hydrostatic pressure approximation provides a "worst-case" scenario and can be used to devise a scale-up strategy to minimize attrition. Additionally, if the bed height is sufficiently high during agitated drying, the particles near the top will experience lower shear stresses than the particles at the bottom. Differences in the mixing of the particle bed would also lead to different residence times of the API particles in the high attrition zones (near the bottom plate and by the vessel walls). These effects can lead to particle-size distributions which are different from what might be estimated from the workflow proposed here. Nonetheless, the proposed workflow provides a platform that can inform the design of the agitated drying operations from fundamental knowledge of the API powder rheology and the propensity of the API particles to break.

Conclusions

API agitation studies at the laboratory scale were performed using a modified setup that reproduced the range of hydrostatic pressures observed during scale-up of agitated drying. Torque profiles as a function of time were recorded for agitation of dry and solvent wet powder beds for a test material API. For dry powder beds, the torque signal increased with time until steady state was reached. The increase in torque was associated with breakage of the "rod-like" API particles which, in turn, led to densification of the powder bed. A 60% reduction in the mean particle size was observed for the dry API. As the blades move through the powder bed, the long aspect ratio particles break normal to the main axis, leading to shorter particles which can pack better. The plateau of the torque signal was found to correlate to the end of the particle breakage process. Torque values were found to increase with hydrostatic pressure but were independent of agitation rate for RPM values ranging from 10–100 RPM. Using the laboratory setup, we were able to match the particle-size distribution observed at the pilot plant scale for the test material API by matching the hydrostatic pressure and number of blade passes experienced at scale.

Particle attrition of solvent wet API powders was significantly lower that what was observed for the dry API. The lower degree of attrition resulted in significantly lower torque values during agitation of the wet API powders when compared to the dry powder. The degree of attrition observed post agitation in wet API increased as the solvent content decreased. These results suggest that the liquid phase could lubricate the powder bed, thus decreasing interparticle friction and reducing the tendency for wet API particles to break. Additionally, the formation of agglomerates was observed during agitation of the wet API. The "rod-like" particles stacked up along the main axis forming "thicker" agglomerates that we hypothesize reduced the tendency for the primary particles to break.

Several characteristics of our API powder beds during agitation were found to be consistent with the behavior of particulate flows in the quasi-static regime. Rheological measurements of dry and wet API powders were performed using the laboratory unit. The rheology of the API powder was found to be in agreement with the predictions from Coulomb's law of friction, where shear stress scales linearly with the normal stress times a proportionality constant called the bulk friction coefficient. In this study, bulk friction coefficients were found to be dependent on the solvent content of the API powder. The bulk friction coefficient of the dry API was significantly higher than the values measured for solvent wet API. This observation further suggests a lubrication effect due to the presence of the liquid phase during

agitation of wet API. Finally, the resulting particle size from several agitation studies was correlated to the amount of work done by the impeller blade to yield an attrition kinetics curve for the test material API. The degree of attrition observed over a large range of experimental conditions collapsed into a single curve which can predict the mean particle size of the API after agitation for wet and dry materials. A proposed workflow for designing agitated drying processes at scale from laboratory measurements was also described. This workflow uses the bulk friction coefficient measurements to predict the amount of torque to be generated during the drying operation at scale. From the torque prediction, the total amount of work done by the impeller can be estimated. The expected particle size from a particular agitated drying process can then be obtained from the attrition kinetics curve measured in the laboratory. Although this workflow may not predict the particle-size distribution for all equipment configurations and API materials, it provides a platform for the design of the agitated drying operations from knowledge of fundamental material properties. This is an improvement from the current trial-and-error approach commonly used in the pharmaceutical industry.

Acknowledgments

The authors would like to thank M. Mahoney for her assistance with particle size measurements of the API powders. Additionally, the authors would like to acknowledge the unpublished work done at Bristol-Myers Squibb by S. Chan and D. Hsieh advancing the concept of pressure onto API powder properties. Finally, we thank J. Tom and J. Tabora for insightful discussion throughout the course of this work.

Literature Cited

1. Paul EL, Tung H-H, Midler M. Organic crystallization processes. *Powder Technol*. 2005;150(2):133–143.
2. Ansel HC, Allen LV, Popovich NG. Dosage form design: pharmaceutical and formulation considerations. In: Troy DB, editor. *Ansel's Pharmaceutical Dosage Forms and Drug Delivery Systems*, 9th ed. Baltimore, MD: Wolters Kluwer, 2005.
3. Seibert KD, Collins PC, Fisher E. Milling Operations in the Pharmaceutical Industry. In: *Chemical Engineering in the Pharmaceutical Industry*. Hoboken, NJ: Wiley, 2011:365–378.
4. Mazzarotta B, Di Cave S, Bonifazi G. Influence of time on crystal attrition in a stirred vessel. *AIChE J*. 1996;42(12):3554–3558.
5. Neil AU, Bridgwater J. Attrition of particulate solids under shear. *Powder Technol*. 1994;80(3):207–219.
6. Murugesan S, Sharma PK, Tabora JE. Design of Filtration and Drying Operations. In: *Chemical Engineering in the Pharmaceutical Industry*. Hoboken, NJ: Wiley, 2011:315–345.
7. Kowalski SJ, Rajewska K, Rybicki A. Destruction of wet materials by drying. *Chem Eng Sci*. 2000;55(23):5755–5762.
8. Lekhal A, Girard KP, Brown MA, Kiang S, Glasser BJ, Khinast JG. Impact of agitated drying on crystal morphology: KCl-water system. *Powder Technol*. 2003;132(2–3):119–130.
9. Remy B, Khinast JG, Glasser BJ. Wet granular flows in a bladed mixer: experiments and simulations of monodisperse spheres. *AIChE J*. 2012;58(11):3354–3369.
10. Lekhal A, Conway SL, Glasser BJ, Khinast JG. Characterization of granular flow of wet solids in a bladed mixer. *AIChE J*. 2006;52(8):2757–2766.
11. Lee T, Lee J. Particle attrition by particle-surface friction in dryers. *Pharm Technol*. 2003;27(5):64–72.
12. Chandratilleke GR, Zhou YC, Yu AB, Bridgwater J. Effect of blade speed on granular flow and mixing in a cylindrical mixer. *Ind Eng Chem Res*.49(11):5467–5478.
13. Stewart RL, Bridgwater J, Zhou YC, Yu AB. Simulated and measured flow of granules in a bladed mixer–a detailed comparison. *Chem Eng Sci*. 2001;56(19):5457–5471.
14. Zhou YC, Yu AB, Stewart RL, Bridgwater J. Microdynamic analysis of the particle flow in a cylindrical bladed mixer. *Chem Eng Sci*. 2004;59(6):1343–1364.
15. Lekhal A, Girard KP, Brown MA, Kiang S, Khinast JG, Glasser BJ. The effect of agitated drying on the morphology of -threonine (needle-like) crystals. *Int J Pharm*. 2004;270(1–2):263–277.
16. Duran J. The static properties of a granular pile. In: Lam L, Langevin D, editors. *Sands, Powders and Grains*, 1st ed. New York: Springer, 1999:54–75.
17. Remy B, Khinast JG, Glasser BJ. The effect of mixer properties and fill level on granular flow in a bladed mixer. *AIChE J*. 2010;56(2):336–353.
18. Lamberto DJ, Cohen B, Marencic J, Miranda C, Petrova R, Sierra L. Laboratory methods for assessing API sensitivity to mechanical stress during agitated drying. *Chem Eng Sci*. 2011;66(17):3868–3875.
19. am Ende D, Birch M, Brenek SJ, Maloney MT. Development and application of laboratory tools to predict particle properties upon scale-up in agitated filter-dryers. *Org Process Res Dev*. 2013;17:1345–1358.
20. Darelius A, Lennartsson E, Rasmuson A, Bjorn IN, Folestad S. Measurement of the velocity field and frictional properties of wet masses in a high shear mixer. *Chem Eng Sci*. 2007;62(9):2366–2374.
21. Remy B, Khinast JG, Glasser BJ. Discrete element simulation of free flowing grains in a four-bladed mixer. *AIChE J*. 2009;55(8):2035–2048.
22. Campbell CS. Rapid granular flows. *Ann Rev Fluid Mech*. 1990;22:57–92.
23. Campbell CS. Granular shear flows at the elastic limit. *J. Fluid Mech*. 2002;465:261–291.
24. Jackson R. Some features of the flow of granular materials and aerated granular materials. *J Rheol*. 1985;30(5):907–930.
25. Remy B. *Granular Flow, Segregation and Agglomeration in Bladed Mixers*. New Brunswick: Chemical and Biochemical Engineering, Rutgers, The State University of New Jersey, 2010.
26. Karmakar S, Kushwaha RL. Development and laboratory evaluation of a rheometer for soil visco-plastic parameters. *J Terramech*. 2007;44(2):197–204.
27. Rognon PG, Roux JN, Naaim M, Chevoir F. Dense flows of cohesive granular materials. *J Fluid Mech*. 2008;596:21–47.

Manuscript received June 16, 2014, and revision received Sep. 15, 2014.